

Characterization of the Unfolding of Ribonuclease A by a Pulsed Hydrogen Exchange Study: Evidence for Competing Pathways for Unfolding[†]

Juhi Juneja and Jayant B. Udgaonkar*

National Centre for Biological Sciences, Tata Institute of Fundamental Research, GKVK Campus, Bangalore 560 065, India

Received July 16, 2001; Revised Manuscript Received December 19, 2001

ABSTRACT: The unfolding of ribonuclease A was studied in 5.2 M guanidine hydrochloride at pH 8 and 10 °C using multiple optical probes, native-state hydrogen exchange (HX), and pulse labeling by hydrogen exchange. First, native-state HX studies were used to demonstrate that the protein exists in two slowly interconverting forms under equilibrium native conditions: a predominant exchange-incompetent N form and an alternative ensemble of conformations, N_I^* , in which some amide hydrogens are fully exposed to exchange. Pulsed HX studies indicated that, during unfolding, the rates of exposure to exchange with solvent protons were similar for all backbone NH probe protons. It is shown that two parallel routes of unfolding are available to the predominant N conformation as soon as it encounters strong unfolding conditions. A fraction of molecules appears to rapidly form N_I^* on one route. On the other route an exchange-incompetent intermediate state ensemble, I_U^2 , is formed. The kinetics of unfolding measured by far-UV circular dichroism (CD) were faster than those measured by near-UV CD and intrinsic tyrosine fluorescence of the protein. The logarithms of the rate constants of the unfolding reaction measured by all three optical probes also showed a nonlinear dependence on GdnHCl concentration. All of the data suggest that N_I^* and I_U^2 are natively like in their secondary and tertiary structures. While N_I^* unfolds directly to the fully exchange-competent unfolded state (U), I_U^2 forms another intermediate I_U^3 which then unfolds to U. I_U^3 is devoid of all native α -helical secondary structure and has only 30% of the tertiary interactions still intact. Since the rates of global unfolding measured by near-UV CD and fluorescence agree well with the rates of exposure determined for all of the backbone NH probe protons, it appears that the rate-limiting step for the unfolding of RNase A is the dissolution of the entire native tertiary structure and penetration of water into the hydrophobic core.

The “new view” of protein folding replaces the concept of folding pathways with that of energy landscapes (1–4). According to the classical view, under conditions where the native conformation is most stable, all unfolded protein molecules fold via essentially the same sequence of events to reach the native state. The new view envisages the concept of parallel events in which each unfolded molecule follows its own trajectory down the free energy landscape to reach the native conformation which resides at the global minimum in free energy. It derives from experimental observations using techniques which give structural information at the atomic level of the protein molecule, such as hydrogen exchange coupled with NMR¹ or mass spectrometry (5–9).

Statistical mechanical models of folding based on lattice model representations of chain geometry, flexibility, and intrachain interactions (10, 11) also support the view that the denatured, transition, and intermediate states are macroscopic forms, which really are distributions of individual

chain conformations. Since the ensemble of unfolded molecules has the highest conformational entropy, a large energy landscape is initially available for these molecules to fold. Some molecules follow a throughway folding trajectory to the native conformation (two-state transition), while other molecules may get transiently trapped in some local energy minima conformations. The latter then must climb energy barriers, that is, break some favorable contacts, to again start moving toward the global energy minimum (multistate kinetics). Most experimental studies of protein folding involve characterization of intermediate conformations of the protein as it folds. Kinetic intermediates accumulate only if they precede a high free energy barrier (transition state), i.e., the rate-determining step of the refolding reaction. A few proteins, for example, chymotrypsin inhibitor 2 (12), the N-terminal domain of λ repressor (13), and CspB (14), have been shown experimentally to fold very rapidly in an apparent two-state manner without populating any intermediates. Many other proteins studied, including RNase A (15, 16), hen egg white lysozyme (17, 18), and barstar (19), undergo multistep folding reactions.

Statistical models suggest that complex energy landscapes are likely to be available for unfolding as well (2, 3). Molecular dynamic (MD) simulations of a number of proteins have also shown that unfolding is a noncooperative process. For example, MD simulations have been able to trap a molten

[†] This work was funded by the Tata Institute of Fundamental Research and the Wellcome Trust. J.B.U. is the recipient of a Swarnajayanti Fellowship from the Government of India.

* To whom correspondence may be addressed. E-mail: jayant@ncbs.res.in. Tel: 91-80-3636422. Fax: 91-80-3636662.

¹ Abbreviations: RNase A, ribonuclease A; NMR, nuclear magnetic resonance; HX, hydrogen exchange; TOCSY, total correlation spectroscopy; pH*, pH of D₂O solutions uncorrected for isotope effects; GdnHCl, guanidine hydrochloride.

globule-like intermediate for hen lysozyme (20) and, recently, for human α -lactalbumin (21). In the latter study, by using a novel MD simulation approach, Paci et al. were able to generate and probe the properties of non-native conformations formed during unfolding, which are consistent with experimental data. The results also showed that the two domains in the molten globule of α -lactalbumin unfold noncooperatively, in agreement with inferences drawn from NMR experiments. An intermediate found in high-temperature unfolding simulations of barnase was seen to have characteristics similar to the refolding intermediate studied by protein engineering and NMR (22).

Until a few years ago, it was believed that kinetic intermediates could not accumulate during unfolding because of their low stability under strongly denaturing conditions. The other reason was that multiple probes had not been used typically to study protein unfolding reactions. Kinetic unfolding intermediates have now been shown to exist for ribonuclease A (23, 24), *Escherichia coli* DHFR (25), and barstar (26–28). Recently, the technique of native-state amide hydrogen exchange has allowed the characterization of small populations of partially unfolded molecules present under subdenaturing conditions. These equilibrium HX studies have shown that partially unfolded forms or unfolding intermediates are populated transiently for several proteins including cytochrome *c* (29), RNase H (30), and barstar (31). Structural characterization of unfolding intermediates gives information about the transition state of unfolding, which is believed to lie close to the native state (32–34).

Ribonuclease A (RNase A), a 124 amino acid protein, has been a model system for protein folding studies for many years. Its refolding has been characterized extensively under various conditions using NMR and several other biophysical techniques (reviewed in ref 39). While the technique of pulse labeling by HX coupled with NMR has been used extensively to study the folding of RNase A and many other proteins and has yielded the most detailed structural models of kinetic folding intermediates (15, 17, 35, 36), the technique has not been used so far to study the unfolding of any protein. Here, this technique is used, for the first time, to obtain residue-specific information about the unfolding of RNase A.

In this method, folded RNase A with deuterium atoms at all amide sites is allowed to unfold for various lengths of time before being given a short (5 s) pulse of protons at alkaline pH. The protons that still have their hydrogen bonds intact or are buried remain protected from exchange, and only those whose hydrogen bonds have broken exchange rapidly with the solvent protons. The protein is then allowed to refold completely to prevent further hydrogen exchange. The structure of the protein at the time of the pulse is therefore imprinted in the extent of proton exchange and can be detected by NMR. The pulse-labeling method of HX therefore allows the direct measurement of the unfolding kinetics of all of the probe protons in RNase A, unlike a competition labeling method employed earlier (40), in which HX rates are measured at each amide site and the mechanism of exchange is critical to the interpretation of the data.

Our data show that all of the observable backbone amide protons have a similar rate of exposure to solvent during the unfolding of the predominant N conformation of RNase A. A few protons, however, show 35–60% burst-phase exposure to labeling. This indicates that a fraction of the

native molecules rapidly goes into an intermediate state, N_I^* , in which some amide sites are exposed to exchange with solvent protons. The rest of the molecules form an exchange-incompetent intermediate state on a parallel route. A comparison of the pulse-labeling studies to CD and fluorescence measurements of unfolding indicates that both of these intermediate ensembles are native-like in their secondary and tertiary structures. The exchange-incompetent intermediate forms another intermediate which has no native far-UV CD signal and has lost some of the fluorescence and near-UV CD signal. All backbone amide protons appear to be still protected from exchange in this intermediate. It finally forms the fully exchange-competent unfolded state as water molecules penetrate the core and the entire structure opens out. Native-state HX studies have also been done on RNase A in the absence of denaturant. The observations from these experiments suggest that, under native conditions, the N conformation is in slow equilibrium with the same partially exchange-competent intermediate, N_I^* , that accumulates initially on one of the two competing pathways of unfolding in high GdnHCl.

MATERIALS AND METHODS

Materials. Bovine pancreatic RNase A (type X11A) was purchased from Sigma Chemical Co. Since the protein was found to be <85% pure, it was further purified by anion-exchange chromatography using the Resource S column from Pharmacia Biotech. The protein used for all experiments was >95% pure. D₂O (99.9% D), DCl, and NaOD were from Sigma. All chemicals used in the experiments were of ultrapure grade from either Gibco BRL or Sigma.

Deuteration of RNase A and GdnHCl. RNase A was deuterated by dissolving the purified lyophilized protein in D₂O at pH 3 and then heating the solution to 68 °C for 45 min. The protein was refolded on ice and lyophilized. The procedure was carried out three times to ensure complete deuteration of all backbone amide protons. A two-dimensional TOCSY spectrum was collected to ensure that the protein was completely deuterated. GdnHCl was deuterated by dissolving it in D₂O and lyophilizing; this was done three times.

Unfolding of RNase A Monitored by Pulse Labeling by HX. Native deuterated RNase A was dissolved (~25 mg/mL) in native buffer (50 mM Tris-HCl/D₂O, pH* 8) and incubated for 8–10 h at 10 °C. Unfolding of the protein was initiated by diluting it into unfolding buffer so that the final unfolding conditions were 5.2 M GdnDCl/50 mM Tris-HCl/100% D₂O, pH* 8. After different times of unfolding, the protein was diluted 10-fold into exchange buffer (5.2 M GdnHCl/50 mM Tris-HCl/H₂O, pH 8). The final exchange conditions were 5.2 M GdnHCl/50 mM Tris-HCl/90% H₂O, pH 8. After a 5 s exchange pulse, the reaction was quenched by 10-fold dilution into low pH (100 mM sodium formate/100% H₂O, pH 3) on ice. Under these conditions RNase A refolds rapidly to its native conformation. Following this protocol, RNase A was labeled at various times of unfolding between 0 and 800 s. For the zero time point, native deuterated protein was directly diluted into the exchange buffer so that unfolding and exchange were initiated simultaneously. All the unfolding/exchange experiments were done at 10 °C by manual mixing. The mixing dead time in these experiments was 10 s.

The proton labeling by HX was also checked at the zero time point at pH 9. The same protocol was followed as described above except that the exchange buffer was at pH 9.

The labeled protein samples were desalted and concentrated using an Amicon YM 3 ultrafiltration membrane. The solvent was finally exchanged to D₂O, pH* 3.5, using Centricon 10 microconcentration tubes. During this time, the protein solution was at pH 3, 8 °C. For all samples the processing time was same (about 4 days). The final pH* was adjusted to 3.5, and the samples were then kept frozen at -20 °C until NMR spectra were collected.

To correct for any labeling occurring at pH 3 during desalting and concentration of the samples, important control experiments were done. In these, the protocol followed was the same as that for the pulse-labeled unfolding experiment, except that the protein was kept all along in deuterated native buffer, before being finally diluted into quench buffer at pH 3. In one control experiment, the solution contained 0.52 M GdnHCl after quenching at pH 3: this control was used for the unfolding experiments (see below). In the other control experiment, the solution did not contain any GdnHCl after quenching: this was used for the native-state HX experiments (see below). The volumes of the solutions in the control experiments were identical to those in the unfolding or native-state HX experiments. The control samples were then processed in exactly the same way as the pulse-labeled samples.

In another control experiment, protonated protein in the same volume at pH 3 was processed in exactly the same way as the pulse-labeled samples. This allowed the proton occupancies of 90% protonated sites to be compared to the proton occupancies measured after labeling at 800 s of unfolding. The latter values were found to be within $\pm 15\%$ of the former.

NMR Measurement and Data Analysis. Two-dimensional ¹H TOCSY spectra of the labeled samples were collected on a Varian 600 MHz NMR spectrometer. Presaturation of the water signal was used for water suppression. Each TOCSY spectrum was collected with 2048 data points along the *t*₂ domain and 512 data points along the *t*₁ domain. A total of 16 scans were collected at each *t*₁ point. A spectral width of 7000 Hz was used, and spectra were collected at 30 °C. The acquisition time for each TOCSY spectrum was about 4 h. Before Fourier transformation, sinebell squared window functions, using phase shifts of 60° were applied to data in both dimensions, and the data were also zero-filled. The amide proton peaks were assigned according to the published proton chemical shifts of RNase A (41). Cross-peak intensities were analyzed using the Felix 97 software. For each TOCSY spectrum, the intensities of the nonexchangeable aromatic ring protons of Tyr76 and Tyr115 were used as internal references. The intensity of each C_αH-NH cross-peak was divided by the sum of the intensities of the reference cross-peaks. Each amide proton site was considered to be fully exchanged with the solvent protons at the longest unfolding time of 800 s. Thus, the normalized intensity of a backbone amide proton in the 800 s unfolded protein spectrum was taken as 100% occupancy at that amide site, and intensities at all other time points were calculated with respect to that. Plots of proton occupancy versus the time of unfolding were made for each proton, and the data were fitted

to a single-exponential equation. The proton intensities were corrected for any labeling occurring at pH 3 while the samples were being desalted and concentrated before being frozen by subtracting out the proton intensities measured in the control experiments described above.

Native-State Hydrogen Exchange. In these HX experiments, the same protocol was used as in the unfolding experiments. Native deuterated RNase A was dissolved in native buffer (50 mM Tris-HCl/D₂O, pH* 8) and incubated at 10 °C for 8–10 h. It was then diluted 10-fold into exchange buffer (50 mM Tris-HCl/H₂O, pH 8). After different times of exchange, ranging from 5 to 1500 s, the reaction was quenched by 10-fold dilution into quench buffer at pH 3 on ice. All of these HX experiments were also done at 10 °C by manual mixing. The labeled samples were desalted and concentrated as above and kept frozen until NMR measurement. ¹H TOCSY spectra of these samples were collected using the same data acquisition parameters as above and the data analyzed similarly. For each amide site, the proton occupancy was normalized, taking the intensity of that proton in the 800 s unfolded spectrum as 100%. The proton intensities were corrected for any labeling occurring at pH 3 while processing of the samples by subtracting out the proton intensities measured in the control experiments described above.

Dynamic light scattering experiments were carried out on a DynaPro-99 machine (Protein Solutions Ltd.) to show that RNase A is monomeric at a concentration of 2 mM (data not shown), which is the initial concentration used in the pulse-labeling unfolding experiments.

Unfolding of RNase A Monitored by Circular Dichroism and Fluorescence. The kinetics of unfolding of RNase A were studied by diluting the native protein into unfolding buffer with the final GdnHCl concentration ranging from 4 to 6.2 M in the post-transition zone. Unfolding was monitored using far-UV CD at 222 nm as a probe for secondary structure breakdown and near-UV CD at 275 nm and intrinsic tyrosine fluorescence at 320 nm as probes for melting of the tertiary structure of the protein. All kinetic unfolding experiments were done at 10 \pm 2 °C, using manual mixing, with a mixing dead time of 10 s. The temperature of the solution inside the cuvette was monitored. The buffer used in all experiments was 50 mM Tris-HCl, pH 8.

The far-UV and near-UV CD-monitored unfolding studies were done on a Jasco J720 spectropolarimeter, with the bandwidth set to 1 nm and a response time of 2 s, using protein concentrations of ~ 30 and ~ 60 μ M, respectively, and using cuvettes with path lengths of 0.1 and 1 cm, respectively. Fluorescence studies were done on a Spex DM3000 Fluorolog spectrofluorimeter. For studying the unfolding kinetics of RNase A by fluorescence, the tyrosine residues in the protein were excited at 280 nm, and their emission was monitored at 320 nm. A slit width of 0.37 nm was used for excitation and 10 nm for emission. Measurements were made with a protein concentration of ~ 8 μ M in a 1 cm path-length cuvette.

Equilibrium unfolding of RNase A as a function of GdnHCl concentration was also monitored by far-UV and near-UV CD and by intrinsic tyrosine fluorescence. The protein was incubated for about 5 h at 10 °C prior to measurement. Fluorescence-monitored equilibrium unfolding

curves were determined for fully deuterated protein in D₂O buffer as well as for fully protonated protein in H₂O buffer.

Data Analysis of CD and Fluorescence Experiments. After correction for buffer background signals, the equilibrium data sets obtained by all three probes were normalized with respect to the corresponding signal for the native protein. The native and unfolded baselines were obtained by linear extrapolation and were assumed to be linearly dependent on GdnHCl concentration. The data were fitted to a two-state unfolding model, as described previously (42).

The entire unfolding process was observable by all three optical probes under the conditions of these experiments. The unfolding kinetics in the post-transition region were described by a two-exponential process and fit to the equation:

$$A(t) = A_{\infty} - A_1 \exp(-\lambda_1 t) - A_2 \exp(-\lambda_2 t)$$

where λ_1 and λ_2 are the apparent rate constants of the slow and fast phases and A_1 and A_2 are the respective amplitudes. A_{∞} is the total kinetic amplitude of the unfolding process. The signal at $t = 0$ for each kinetic trace was calculated using the parameters obtained from the fit. The $t = 0$ and $t = \infty$ values were normalized with respect to the native protein signal so that the kinetic data could be directly compared to the equilibrium unfolding transition.

RESULTS

Unfolding Kinetics of RNase A Monitored by CD and Fluorescence. Before pulse labeling by HX methods could be used to study the unfolding of RNase A, it was necessary to use optical probes, which monitor gross secondary and tertiary structures, to define the basic unfolding reaction. Unfolding measured by all three probes, viz., far-UV CD, near-UV CD, and intrinsic tyrosine fluorescence at different GdnHCl concentrations, shows biphasic kinetics. Virtually no burst phase changes are observed, as seen in Figure 1. The figure shows that the equilibrium unfolding transitions of RNase A monitored by CD at 222 and 275 nm and by fluorescence show a C_m of 3.5 M GdnHCl. The kinetic amplitudes of the two observable unfolding phases account for the entire equilibrium amplitude at all GdnHCl concentrations at which unfolding is monitored.

Fractional ellipticity values obtained from raw kinetic traces of CD measured at 222 and 275 nm are shown in Figure 2 to highlight the difference in the kinetics of unfolding of RNase A in 5.2 M GdnHCl vs the almost overlapping kinetics in 4.4 M GdnHCl. The coincidence of far- and near-UV CD-monitored unfolding kinetics of RNase A in 4.5 M GdnHCl at pH 8 and 10 °C has also been reported earlier (23, 40). When monitored by far-UV CD, the kinetics of unfolding in 5.2 M (and also in 4.5 and 6 M) GdnHCl were found to be independent of protein concentration in the range 20–130 μ M (data not shown).

Figure 3 shows the logarithm of the rate constants of the slow phase of unfolding measured by all of the three optical probes. Below 4.5 M GdnHCl, the difference in the rates measured by far-UV CD and the two tertiary structure probes is very small. At concentrations of GdnHCl above 4.5 M, the unfolding rates obtained by far-UV CD diverge from and are about 30–40% faster than the rates observed by near-UV CD. This difference is significant because the errors in our measurements are typically less than 5% and always less

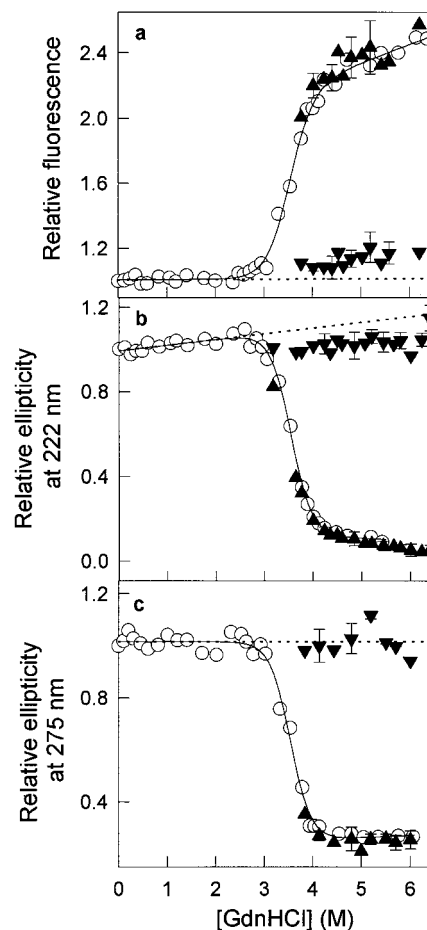


FIGURE 1: Equilibrium and kinetic amplitudes of GdnHCl-induced unfolding of RNase A at pH 8, 10 °C. Unfolding was followed by monitoring (a) the intrinsic tyrosine fluorescence and the mean residue ellipticity (b) at 222 nm and (c) at 275 nm. Tyrosines were excited at 280 nm, and the fluorescence emission was monitored at 320 nm. Symbols: (○) equilibrium unfolding amplitude at different [GdnHCl]; (▲) final amplitude of the kinetic unfolding curve obtained by extrapolation to $t = 4$ using a double-exponential equation; (▼) initial amplitude of the kinetic unfolding curve obtained by extrapolation to $t = 0$ using a double-exponential equation. All amplitudes are relative to a value of 1 for N. The solid lines are fits of the equilibrium unfolding data to a two-state $N \rightleftharpoons U$ model (see text) and yielded values for ΔG_U (in kcal mol⁻¹) and m_G (in kcal mol⁻¹ M⁻¹) equal to (a) 8.2 and -2.3, (b) 9.4 and -2.6, and (c) 9.6 and -2.7. The dotted line in each panel is the estimated value of N obtained by linear extrapolation of the native protein baseline.

than 15% of the reported mean value. Moreover, the rates measured by near-UV CD are identical to those monitored by fluorescence. Thus, the difference between the rates of unfolding measured by secondary and tertiary structure probes is accentuated by both the tertiary structure probes yielding similar rates and their similar dependences on denaturant concentration. Figure 3 also shows that the logarithms of the slow-phase rate constants measured by all three probes have a nonlinear dependence on denaturant concentration. The observation that the kinetics of near-UV change (at 60 μ M protein concentration) and the kinetics of fluorescence change (at 8 μ M protein concentration) are the same indicates that aggregation processes are not significant, in agreement with the observation that far-UV CD kinetics are also independent of protein concentration.

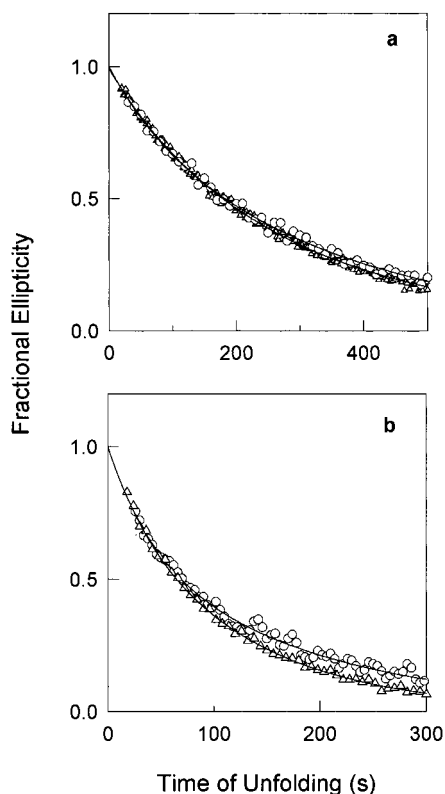


FIGURE 2: Kinetics of unfolding of RNase A monitored by circular dichroism. RNase A was unfolded at 10 °C in 50 mM Tris-HCl, pH 8, in the presence of (a) 4.4 M and (b) 5.2 M GdnHCl. Fractional ellipticities at (Δ) 222 nm and (O) 275 nm are plotted versus time of unfolding. Only the initial parts of the unfolding traces are shown here. The solid lines are two-exponential fits of the observable kinetic process (see text).

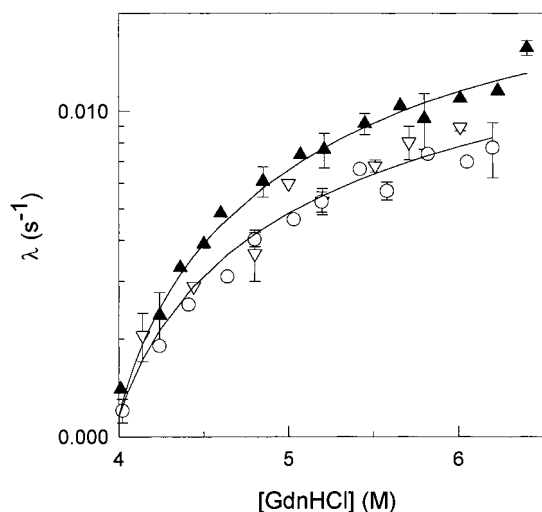


FIGURE 3: Apparent rate constants of the slow observable kinetic phase in GdnHCl-induced unfolding of RNase A at pH 8, 10 °C. Unfolding was monitored by (O) fluorescence, (\blacktriangle) far-UV CD, and (∇) near-UV CD. Dependences of the apparent rate constants of the slow phase, λ , on [GdnHCl] are shown here. The solid lines through the data points have been drawn by inspection only. Each data point represents the mean value obtained from three separate repetitions of the experiment. For most of the data points, error bars are smaller than the size of the symbols.

The faster phase accounts for $30 \pm 10\%$ of the total amplitude change during unfolding. The rate constants of the faster phase of unfolding, observed by all three spectroscopic probes, are similar ($0.02 \pm 0.009 \text{ s}^{-1}$) and almost

independent of GdnHCl concentration (data not shown). These are characteristics of the phase which arises due to proline isomerization and have been reported earlier (16, 43–46). Above pH 4.5, the proline isomerization step is known to be coupled to the structural transition during unfolding (43). The unfolding process monitored by far- and near-UV CD has also previously been observed to be biphasic (40, 47, 48) and the faster phase shown to arise from the $U_F \rightleftharpoons U_S$ step of unfolding (40). U_F comprises the population of unfolded molecules with X-Pro bonds in the native cis conformation, and U_S molecules have one or both X-Pro bonds in the trans conformation.

Since the optical experiments were carried out with protonated protein in H_2O buffer, while the pulse labeling by HX experiments (see below) were carried out with deuterated protein in D_2O buffer, it was important to determine whether the replacement of deuterium for amide proton affected the stability of the protein as well as its unfolding kinetics. A fluorescence-monitored equilibrium unfolding curve of deuterated protein in D_2O was found to overlap completely with that of protonated protein in H_2O (data not shown). Similarly, the fluorescence-monitored unfolding rates of deuterated protein in D_2O buffer were found to be identical, within experimental error, to those of protonated protein in H_2O buffer (unpublished data), over the entire range of GdnHCl concentration studied (Figure 3). Thus, isotope effects play no significant role in determining the stability or unfolding kinetics of RNase A, and the kinetics of unfolding determined by optical methods in H_2O buffer can be directly compared to the kinetics of unfolding determined from pulse-labeling HX studies carried out in D_2O buffer.

Exposure of Backbone Amide Protons of RNase A during Unfolding. Completely deuterated RNase A at pH* 8 was unfolded in 5.2 M GdnDCI. Figure 4 shows the 1D cross sections of three amide proton cross-peaks in the fingerprint region of TOCSY spectra of RNase A, obtained for samples that were unfolded for 0, 40, 250, and 800 s, before being given a 5 s pulse of exchange. While Cys72 shows 9% labeling, Lys61 and Glu49, respectively, show 30% and 50% labeling even at the zero time of unfolding. About 43 amide protons were well resolved in the spectra, and proton occupancies and the kinetics of exposure for all of these could be evaluated. The peak intensities increase with time of unfolding, as is expected and clearly evident in Figure 4. The figure shows cross-peak intensities measured in one experiment.

The intrinsic amide proton exchange reaction in unfolded RNase A has a time constant of 35 ms at pH 8 and 10 °C. Thus, if exchange during the 5 s pulse occurs by the EX2 mechanism, any form with protons having a protection factor of <150 , including completely unfolded protein, will also show labeling. If HX during the 5 s pulse occurs only by the EX1 mechanism, as expected under the experimental conditions used, then any native molecules present at the time of application of the pulse will not get labeled during the duration of the pulse because it unfolds at a rate of about 0.005 s^{-1} . Thus, the pulsed HX methodology directly measures the unfolding kinetics of RNase A. The kinetics of deprotection of six amide protons followed as a function of the unfolding time are shown in Figure 5. The cross-peak intensity of an amide proton at a particular time of unfolding

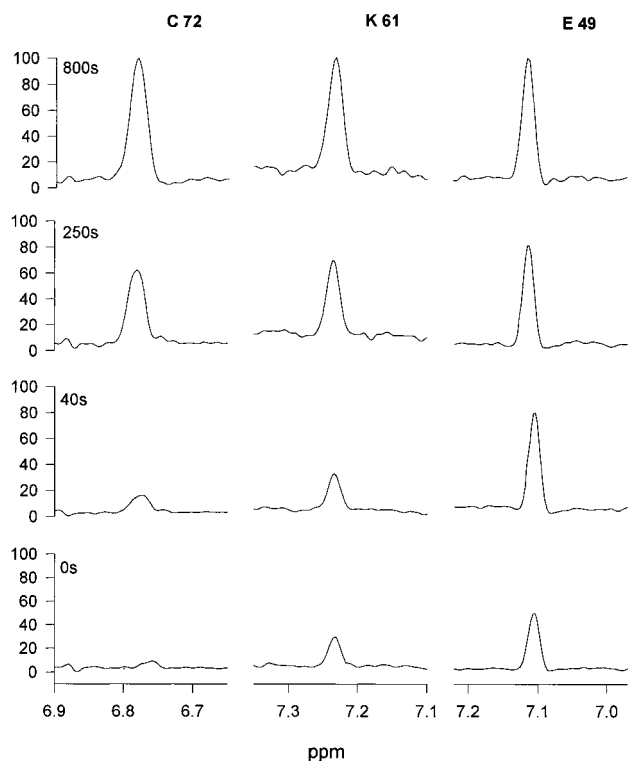


FIGURE 4: One-dimensional cross sections of $C_{\alpha}H-NH$ cross-peaks of RNase A. The peak amplitudes of three residues, belonging to class I (Cys72) and class II (Lys61 and Glu49) (see Table 1 for classification of protons), are shown at four different times of unfolding. The amplitudes at all unfolding times are plotted, taking the amplitude of that peak at 800 s to be 100%. All intensities have been internally normalized to nonexchangeable tyrosine ring protons and corrected for any labeling at pH 3 (see text): Cys72 did not show any labeling, while Lys61 was corrected for 19% and Glu49 for 46% labeling in the pH 3 control.

represents the fraction of molecules in the population, in which the amide proton has exchanged with solvent water protons. The observed rates of exposure of all the amide protons are plotted versus the primary sequence of the protein, as a histogram in Figure 6a. The 43 probe NH protons are seen to unfold with an average rate constant of $0.005 \pm 0.001 \text{ s}^{-1}$. It is observed that all individual rates of exposure are within three standard deviations ($\pm 0.003 \text{ s}^{-1}$) of the average. Hence, the individual rates of exposure are assumed to be the same.

Proton occupancies of all 43 probe amide protons were calculated as explained earlier. Figure 5 shows that Val63, Tyr97, and His12 show $5 \pm 5\%$, $13 \pm 5\%$, and $16 \pm 10\%$ proton occupancies, respectively, at the start of unfolding; Val43, Gln34, and Glu49 show $50 \pm 2\%$, $61 \pm 12\%$, and $59 \pm 9\%$ burst-phase labeling, respectively. The data represent the averages of three sets of experiments. All reported proton occupancies have been corrected for any labeling that might occur at pH 3 while desalting and concentration of the samples (see Materials and Methods). While 25 of the 43 protons do not show any labeling in the pH 3 control, 11 get labeled to $4 \pm 3\%$, 4 get labeled to $19 \pm 2\%$, and 3 protons show $44 \pm 3\%$ labeling.

The proton occupancy at $t = 0$ for each amide proton was obtained by fitting the HX data to a first-order exponential function. It was observed that 33 out of the 43 observable protons show very little labeling at zero time of unfolding (H occupancy = $9 \pm 4\%$). However, 10 residues show a

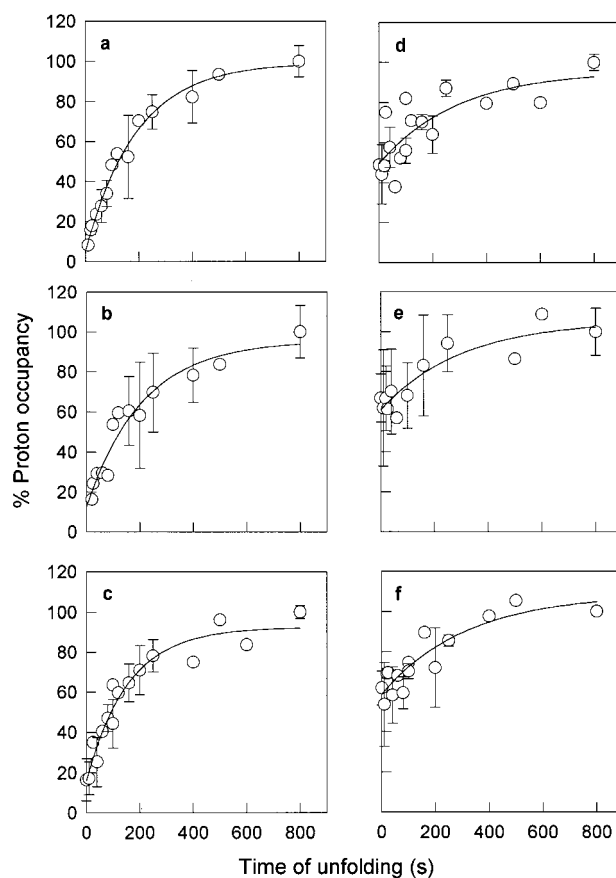


FIGURE 5: Kinetics of exposure of backbone amide deuterons of RNase A. (○) The accessibility to exchange with solvent H_2O protons vs time after initiation of unfolding in 5.2 M GdnHCl at pH* 8 (not corrected for isotope effects), 10°C , is plotted for (a) Val63, (b) Tyr97, (c) His12, (d) Val43, (e) Asn34, and (f) Glu49. The internally normalized intensity of each $C_{\alpha}H-NH$ cross-peak (see text) in the TOCSY spectrum of the longest unfolding time point (800 s) is taken as 100% proton occupancy of that amide proton site. All other intensities are normalized to this. The solid line in each panel is a single-exponential fit of proton occupancies versus the unfolding time. The mean rate of exposure of 43 probe protons is 0.005 s^{-1} and the standard deviation is 0.001 s^{-1} . Proton occupancies of all amide protons have been corrected for labeling in the pH 3 control sample (see text): His12 was corrected for 5%, Val43 for 41%, Asn34 for 21%, and Glu49 for 46% labeling in pH 3. Val63 and Tyr97 showed no labeling in the pH 3 control sample.

proton occupancy of $47 \pm 9\%$ at $t = 0$ unfolding time. Accordingly, the protons have been classified into two groups, class I and class II, on the basis of their proton occupancies at $t = 0$ unfolding time, as shown in Table 1. Figure 6b shows a ribbon diagram of the RNase A structure with the residues belonging to class I and class II marked in different colors.

The extents of labeling of the backbone NH protons at the $t = 0$ unfolding time were the same when a 5 s exchange pulse was given at pH 9, instead of at pH 8 (data not shown).

Thus, in 5.2 M GdnHCl, the rate constant of the slow phase of unfolding measured by far-UV CD at 222 nm, a probe for α -helical secondary structure, is $0.008 \pm 0.001 \text{ s}^{-1}$. The rate constants observed by the two tertiary structure optical probes, near-UV CD, and fluorescence agree well and are $0.005 \pm 0.0005 \text{ s}^{-1}$ and $0.005 \pm 0.0004 \text{ s}^{-1}$, respectively. The rate of exposure of amide protons to HX is $0.005 \pm 0.001 \text{ s}^{-1}$, which is the same as what is observed by the two

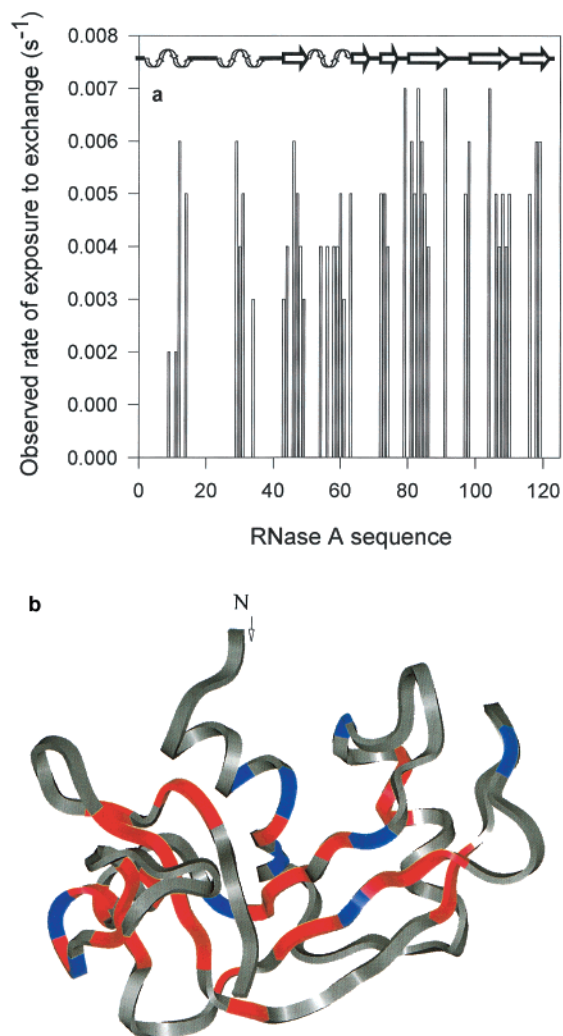


FIGURE 6: (a) Rates of exposure of backbone amide sites observed by pulse-labeled hydrogen exchange. The increase in proton occupancy as a function of unfolding time for each amide proton was fit to a single-exponential equation. Rate constants obtained from such fits are plotted against the RNase A primary sequence. (b) Location of amide proton probes used to study the unfolding pathway of RNase A. The residues in red belong to class I and the residues in blue belong to class II and show $9 \pm 4\%$ labeling and $47 \pm 9\%$ labeling at $t = 0$ unfolding time, respectively. The RNase A figure was drawn using MOLSCRIPT from the protein NMR structure 2AAS submitted by Santoro et al. in the PDB (53).

tertiary structure probes and slower than the rate of α -helical secondary structure dissolution.

Native-State HX Studies. HX experiments were done in the absence of denaturant at pH 8 and 10 °C, as described above. Plots of proton occupancies versus length of the exchange pulse, from these experiments, for three residues are shown in Figure 7. The native-state HX data are plotted along with the unfolding data for these residues. Proton occupancies measured at the earliest time point, that is, 5 s, in the HX experiments under native conditions are listed in Table 1. It is seen that virtually all of the amide sites that are labeled to any significant extent belong to the class II residues and that the extent of labeling (standard deviation of $\pm 20\%$) in the native-state HX experiments is either similar to or lower than that at the start of unfolding in 5.2 M GdnHCl. For 7 protons, the extent of labeling varies from 20% to 60% and does not change when the time for which

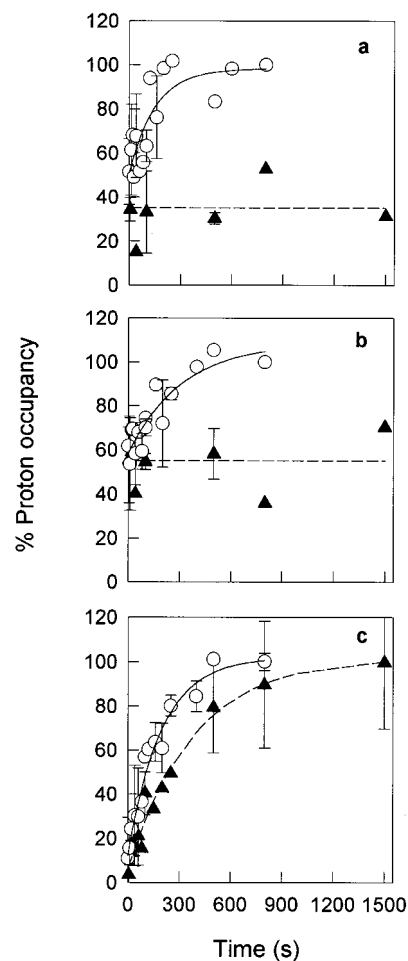


FIGURE 7: Representative native-state HX kinetics of RNase A amide protons. Native protein in 50 mM Tris-DCl, pH* 8 at 10 °C, was allowed to exchange with solvent H₂O protons for increasing lengths of time (see text). (▲) Extent of labeling of (a) Lys91, (b) Glu49, and (c) Lys31 as a function of time allowed for HX. The dashed line in (a) and (b) has been drawn by inspection and is a single-exponential fit of the native-state labeling data in (c). Also shown are the kinetics of HX during unfolding in 5.2 M GdnHCl, pH 8 and 10 °C, for these protons.

the native protein remains in the exchange buffer is varied in the range 5–1500 s. The class II proton Ser59 and two class I protons, viz., Lys31 and Tyr97, show an increase in proton occupancy from 0% to 100%, as the length of the exchange pulse increases from 5 to 1500 s. Val43 and Lys61, which belong to class II, also show an increase in labeling with more time allowed for native-state HX.

DISCUSSION

CD and Fluorescence-Monitored Unfolding Kinetics. The GdnHCl-induced unfolding of RNase A was studied by measuring the change in the ellipticity at 222 and 275 nm and in the intrinsic tyrosine fluorescence of the protein as it unfolds. These optical probes monitor the global unfolding process. The rate constants of the slower phase of the unfolding reaction, measured by the three spectroscopic probes, are not coincident. The rate constants monitored by far-UV CD, which is a probe for secondary structure, are faster than those measured by near-UV CD and fluorescence, both of which probe the tertiary structure of a protein. The rate constants diverge only above 4.5 M GdnHCl. Coincident kinetics of unfolding of RNase A, monitored by far- and

Table 1: Observed Rates of Exposure of Backbone Amide Protons during Unfolding of RNase A in 5.2 M GdnHCl, pH 8 and 10 °C

amide proton	secondary structure	H-bond acceptor in native RNase A	main chain surface accessibility ^a (%)	proton occupancy at $t = 0$ of unfolding ^b (%)	proton occupancy of native protein ^c (%)	observed rate of exposure (s ⁻¹)	k_{int}^d (s ⁻¹)
Class I							
H 12	helix 1	F8 O	0	16	13 ± 3	0.006	37.5
M 29 ^e	helix 2	Y25 O	1.1	0	0	0.006	46.1
M 30	helix 2	C26 O	0	17	0	0.004	37.5
K 31	helix 2	N27 O	7.9	12	4 ± 5	0.005	35
N 44	β -sheet 1	C84 O	2.1	11	0	0.004	66.6
F 46	β -sheet 1	T82 O	0	11	0	0.006	27.2
V 47	β -sheet 1	H12 O	0	1	11	0.005	6.8
H 48	β -sheet 1	S80 O	26.3	12	0	0.004	17.1
V 54	helix 3	L51 O	0	13	0	0.004	3.9
A 56	helix 3	A52 O	8	10	0	0.004	47.2
C 58	helix 3	Q55 O	7.3	12	0	0.004	76.5
Q 60	helix 3	V57 O	49.9	7	0	0.005	68.2
V 63	β -sheet 2	C72 O	9.9	5	0	0.005	12.4
C 72	β -sheet 2	V63 O	0	11	0	0.005	220.7
Y 73	β -sheet 2	V108 O	0	11	0	0.005	46.1
Q 74	β -sheet 2	K61 O	0	9	0	0.004	38.4
M 79	β -sheet 1	K104 O	0	9	0	0.007	46.1
I 81	β -sheet 1	A102 O	0	8	0	0.006	11.1
T 82	β -sheet 1	F46 O	0	7	0	0.005	14.9
C 84	β -sheet 1	N44 O	0	10	0	0.006	69.8
R 85	β -sheet 1	K98 O	0	10	0	0.005	103.2
E 86	β -sheet 1	P42 O	27.5	6	0	0.004	15.3
Y 97	β -sheet 1	N27 O ^b	15.2	13	0	0.005	16
K 98	β -sheet 1	R85 O	2.9	9	0	0.006	30.5
K 104	β -sheet 1	M79 O	0	0.3	0	0.007	56.7
I 106	β -sheet 2	S75 O ^r	0	6	0	0.005	7.7
I 107	β -sheet 2		0	9	0	0.004	3.3
V 108	β -sheet 2	Y73 O	0	7	12	0.005	3.5
A 109	β -sheet 2	H119 O	0	11	0	0.004	21.6
C 110	β -sheet 2	N71 O	3.2	12	0	0.005	105.7
V 116	β -sheet 2	E111 O	0	7	0	0.005	6.7
V 118	β -sheet 2	A109 O	0.2	0	0	0.006	3.4
H 119	β -sheet 2	A109 O	0	9	0	0.006	17.1
Class II							
E 9 ^e	helix 1	A5 O	13.5	43	0	0.002	10.6
Q 11 ^e	helix 1	K7 O	0	35	0	0.002	56.7
D 14	loop	V47 O	0	46	16 ± 16	0.005	19.2
N 34	helix 2	K31 O	0.2	61	79 ± 1	0.003	152.7
V 43	β -sheet 1	none	14.4	50	49 ± 4	0.003	3.4
E 49	loop	none	0	59	56 ± 20	0.003	12.7
S 59	helix 3	A56 O	69.3	35	0	0.004	201.3
K 61	β -sheet 2	Q74 O	0	44	16 ± 16	0.003	43
D 83	β -sheet 1	T100 O	0.5	41	26 ± 11	0.007	23.7
K 91	loop		0	51	34 ± 5	0.007	54.2

^a Calculated using the protein solvent accessibility (PSA) program (70). ^b Proton occupancy at $t = 0$ from single-exponential fits of the kinetics of exposure of NH protons. ^c Proton occupancy in native RNase A after a 5 s exchange pulse. ^d Intrinsic exchange rates of protons in RNase A in pH 8 and 10 °C (71). ^e E 9, Q 11, and M 29 are weak cross-peaks; there is therefore a >20% error in the measurement of rate constants of exposure for these protons.

near-UV CD in 4.5 M GdnHCl had been observed earlier (40). The complete unfolding arm of the chevron of RNase A at pH 8 and 10 °C, however, has not been reported in any previous study. The data clearly indicate that, at concentrations above 4.5 M GdnHCl, α -helical secondary structure breakdown occurs before the entire tertiary structure of the protein dissolves, which suggests the existence of an unfolding intermediate.

The logarithm of the slow-phase rate constants plotted vs GdnHCl concentration also shows a deviation from linearity, as measured by all three probes. This is evidence for transient accumulation of at least one kinetic unfolding intermediate. The slope of such a plot gives the m -value of the transition, which is the difference in the extent of surface area exposed in the two states involved in the transition. At denaturant

concentrations where the intermediate is not populated, the process is effectively two state ($N \rightarrow U$). In this region, the m -value represents the difference in the extent of solvent exposure between the transition state and the native state ($m_{\ddagger} - m_N$). At higher denaturant concentrations where an intermediate, I, is significantly populated, there is a change in the slope of the unfolding arm of the chevron, which defines $m_{\ddagger} - m_I$. Since the intermediate is more stable than the native state at these GdnHCl concentrations, the height of the unfolding barrier increases and the rate of unfolding decreases compared to what it would be without the accumulation of I (27, 38, 49).

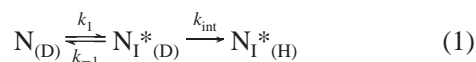
It has been argued that these “rollovers” in chevron plots can arise due to changes in the composition of the transition state ensemble, instead of changes in the ground state from

which folding or unfolding occurs, which might, for instance, be an intermediate formed within the dead time of the experiment (50, 51). For proteins showing burst phase changes during refolding or unfolding, analysis of the spectroscopic properties of the dead time species allows determination of whether the reaction started from the denatured or the native state or whether the initial state has different properties (27, 51). The lack of a burst phase change in the unfolding studies with RNase A presented in this paper does not, however, indicate the absence of an intermediate.

In the case of proteins such as U1A, the curvatures in chevron plots can be accounted for by movements of the transition state ensemble, because all of the kinetic data are compatible with a two-state process (52). It is unlikely that the nonlinearity in the unfolding arm of the chevron of RNase A is due to movements of the transition state ensemble. In fact, the difference in kinetics of unfolding of the α -helical secondary and tertiary structures of the protein, along with the observation of a nonlinear dependence of the logarithm of rate constants on denaturant concentration, strongly suggests that unfolding proceeds in at least two separate reaction steps. The unfolding reaction steps could be consecutive and/or could occur in parallel with or without the population of unfolding intermediates.

Native-State Hydrogen Exchange. Native-state heterogeneity with two or more native states unfolding via parallel pathways would be the simplest explanation for the unfolding kinetics, observed using optical probes. There is, in fact, proton NMR evidence for some amino acid residues in RNase A existing in more than one discrete conformation (53, 54) in solution. Moreover, heteronuclear NMR studies (55) clearly indicate the presence of alternative conformations in addition to the predominant conformation in solution: many extra resonances corresponding to at least 30 spin systems over and above the 119 expected are observed in triple resonance NMR spectra of RNase A. Thus, RNase A appears to exist in at least two conformations in solution: the predominant (and, hence, more stable) N conformation and the alternative ensemble of conformations, N_I , with the equilibrium between N and N_I being slow on the NMR time scale. Since the HX properties of N and N_I are expected to be different, it was important to first determine these using native-state HX studies.

In the native-state HX experiments reported here, it is observed that, even in 0 M GdnHCl at pH 8 and 10 °C, there are a few amide protons which are accessible to hydrogen exchange in RNase A. The extent of labeling of a particular NH site represents the fraction of molecules in which it is exposed to exchange with the solvent protons. The observation that a few protons do get labeled suggests that there is an ensemble of partially unfolded exchange-competent molecules, N_I^* , in slow equilibrium with the native state, N, under native conditions. If the $N \rightleftharpoons N_I^*$ equilibrium were fast, these amide sites would have shown 100% proton occupancy in the absence of denaturant. N_I^* is an ensemble of high-energy conformations with one or a few amide protons exposed to solvent. Thus, native-state HX occurs according to the mechanism:



In this mechanism k_1 is the rate of exposure of an NH proton, k_{-1} is its rate of protection from exchange, and k_{int} is the intrinsic exchange rate of the proton in pH 8 and 10 °C (cf. Table 1). The native-state HX methodology used here will label any exposed NH proton, irrespective of the mechanism of exchange operational under these conditions. The observed rate of hydrogen exchange, k_{ex} , for each proton is given by the equation:

$$k_{\text{ex}} = \frac{k_1 k_{\text{int}}}{k_1 + k_{-1} + k_{\text{int}}}$$

For Lys31, Val43, Ser59, Lys61, and Tyr97, which show an increase in native-state labeling as the time allowed for exchange with solvent water protons is increased from 5 to 1500 s (Figure 7c), k_{ex} must have a value such that exchange is observable in this time range. Indeed, when the HX behavior of these protons was simulated using the program KINSIM (56), k_1 was observed to have a value of $0.002 \pm 0.001 \text{ s}^{-1}$, and k_{-1} was 100 times faster than k_1 . Other protons show 20–60% labeling at the shortest pulse length of 5 s in the native-state HX experiment, and the extent of labeling remains the same up to 1500 s. Thus, k_{ex} for these protons must be too slow to bring about an observable change in proton occupancy in 1500 s. Kinetic simulations of the native-state HX of these protons show that they have a slower k_1 and a faster k_{-1} compared to the NH protons which exhibit an increase in labeling from 5 to 1500 s (Figure 7a,b).

It should be mentioned that Val43 and Ser59 are among the protons classified by Loh et al. as exchanging by the EX2 mechanism at pH 8 and 10 °C (57). The observed rates of exchange of these protons predicted by their simulations agree well with the rates seen in the native-state HX experiments in 0 M GdnHCl, presented here. In previous studies, Val43 and Ser59 were reported to show some degree of labeling in control native RNase A samples which were exposed to a 10 s proton labeling pulse at pH 9 (15).

Most of the residues which are exposed to exchange in the N_I^* ensemble are located in relatively more flexible regions of native RNase A, in loops or at the ends of helices (Figure 6b). Moreover, Val43 and Glu49 are not hydrogen bonded in the native protein (53). The only anomalous behavior is shown by Gln60, which lies at the end of helix 3 but shows only about 20% labeling when the native protein is subjected to a 1500 s labeling pulse.

Pulse Labeling by HX during Unfolding of RNase A. When RNase A is pulse labeled by HX while unfolding in 5.2 M GdnHCl, the observed kinetics of exposure to solvent of the 43 NH probe protons could be fitted to a single-exponential process and showed the same rate constant of about 0.005 s^{-1} , indicating a single global unfolding step. On the basis of just the observed rates of exposure of the NH protons, it would appear that the unfolding of RNase A is a two-state process. There are, however, differences observed in the extents of labeling of a few protons at the start of the unfolding process. Thirty-three of the 43 amide protons, belonging to class I residues, that were evaluated show close to 0% proton occupancy at the zero time of unfolding. Surprisingly, the extents of labeling of a few protons, belonging to class II residues, are clearly nonzero. Glu9, Gln11, Asp14, Asn34, Val43, Glu49, Ser59, Lys61, Asp83, and Lys91 show proton occupancies of $47 \pm 9\%$ at $t = 0$.

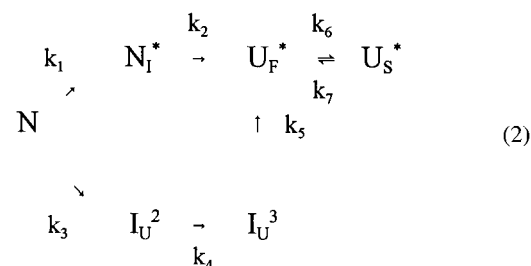
The pattern of labeling seen in the early product of unfolding in 5.2 M GdnHCl is very similar to that seen in N_1^* . All residues that are labeled in N_1^* are labeled in the early product of unfolding (Table 1). Only three of the residues that are labeled in the early product of unfolding (the class II residues) do not appear labeled in N_1^* . For those that are labeled, the extent of labeling in the early product of unfolding is the same or greater than in N_1^* . These results suggest that as soon as RNase A is exposed to strong unfolding conditions, a fraction of N molecules is transformed rapidly to a partially unfolded form that is either identical to N_1^* or to an early product of unfolding of N_1^* whose pattern of labeling is similar to that of N_1^* . Since there is no evidence for the latter possibility, the simplest assumption is that the partially unfolded form is, in fact, N_1^* . Thus, the extent of labeling of the class II residues that occurs rapidly (within the dead time of 10 s for these manual mixing experiments) during unfolding depends on how much N_1^* preexisted prior to the commencement of unfolding and on how much N_1^* forms rapidly from N. It is clear that not all N molecules transform to N_1^* because if that were to happen, then all class II residues would be labeled completely in the initial step of unfolding. Those that do not, must unfold via an alternative, competing pathway on which the initial product is exchange incompetent. It is stressed that N_1^* is not a unique form but represents an ensemble of partly unfolded forms (see above), that the individual members of the ensemble may be exchange competent at any particular class II site to different extents, and that the individual members of the ensemble may form at different rates from N, via parallel or consecutive unfolding reactions.

EX2 vs EX1 Exchange in 5.2 M GdnHCl. In earlier studies, a competition labeling methodology had been used to study the unfolding of RNase A in 4.5 M GdnHCl (40). In those experiments, native deuterated protein at pH* 3.5 was unfolded in 4.5 M GdnHCl/90% H₂O at pH 8 and 10 °C, and the exchange was quenched after different lengths of time by lowering the pH. A major limitation of such a competition labeling method is that the unfolding rate can only be indirectly inferred from the observed HX rates. By the competition labeling method, most of the NH protons were seen to exchange solely by the EX1 mechanism, with similar observed HX rate constants. In addition, seven protons (Met30, Arg33, Asn34, Val43, Ser59, Cys65, and Val124) showed faster rates of exchange, and their HX rates increased when unfolding/exchange was studied at pH 9. Nine more protons became significantly faster than the rest at pH 9, although none of the protons showed the expected 10-fold increase in HX rates. These observations and simulation of the unfolding data using the general two-process model for hydrogen exchange proposed by the authors (57, 58) led them to conclude that these NH protons exchanged by both EX1 and EX2 mechanisms even at GdnHCl concentrations higher than the C_m of unfolding (=3.5 M). None of the residues classified by Loh et al. (57) as exchanging by both EX1 and EX2 mechanisms during unfolding in 4.5 M GdnHCl at pH 8 or 9 show an increase in proton occupancy at the zero time of unfolding at pH 9 in this study. Here, the extent of labeling for a pH 9 pulse was evaluated only at $t = 0$ of unfolding. Since the intrinsic rate of exchange is 10-fold faster at pH 9 than at pH 8 (59), this observation suggests that the contribution of EX2

exchange is minimal and that labeling occurs primarily by EX1 exchange in 5.2 M GdnHCl.

Mechanism of Unfolding of RNase A. The model for unfolding of RNase A in 5.2 M GdnHCl at pH 8 and 10 °C must explain the following experimental observations: (i) Native RNase A comprises at least two populations of molecules, an exchange-incompetent N conformation and an exchange-competent N_1^* conformation ensemble in slow equilibrium with each other. In N_1^* , a few backbone amide sites are fully exposed to HX. Thus, unfolding commences from two preexisting native conformations: the predominant form, N, and the ensemble, N_1^* . (ii) A fraction of N molecules rapidly unfolds to N_1^* , while the remaining N molecules unfold to an exchange-incompetent form via an alternative, competing pathway (see above). (iii) The observable rate of exposure of all of the backbone amide probe protons is similar. (iv) Above 4.5 M GdnHCl, the kinetics for the loss of secondary structure of the protein are not coincident with the unfolding kinetics of the tertiary structure, as measured by CD and intrinsic tyrosine fluorescence of the protein. (v) The logarithms of the rate constants of the slower phase of unfolding, monitored by CD and by fluorescence, have a nonlinear dependence on GdnHCl concentration. (vi) Equilibrium-unfolded RNase A exists in two unfolded forms: 20% of the molecules exist as U_F and 80% as U_S .

To determine the minimal mechanism that will explain all the data, kinetic simulations using the program KINSIM (56) were carried out with progressively more complex mechanisms. The following mechanism of unfolding of N is the minimal one that accounts for the data:



In unfolding conditions, the stabilities of both N and N_1^* are expected to decrease, and the value of k_1 will increase; if it increases significantly relative to the value of k_3 , some preexisting N molecules will form N_1^* . Then, the extent (35–60%) of labeling seen at each of the class II amide hydrogen sites, at 10 s of unfolding in 5.2 M GdnHCl, will depend on the fraction of preexisting N_1^* molecules as well as on that which forms rapidly within this time from N.

All reactions in mechanism 2 operate in both the forward and backward directions. Under the strong denaturing conditions of the experiments, the backward (folding) reactions are, however, expected to be much slower than the unfolding reactions and have therefore been ignored in mechanism 2. Not only must the rates of the backward transitions $N_1^* \rightarrow N$ and $I_U^2 \rightarrow N$ be slower than k_1 and k_3 but they must also be less than k_2 , k_4 , and k_5 ; otherwise, all protein molecules will show proton labeling at all amide sites in the burst phase.

Since N_1^* represents an ensemble of partially unfolded forms, the value of k_1 may be different for the formation of

each member of the ensemble (see above), and any estimated value of k_1 for the exposure of any one class II amide hydrogen site would, in fact, represent the effective rate of formation of all members of the N_1^* ensemble in which that particular amide hydrogen site is exposed. According to mechanism 2, N_1^* and I_U^2 accumulate rapidly, in the 10 s dead time of the HX experiment, on two competing routes when N encounters strong denaturing conditions. Unlike N_1^* , I_U^2 is an exchange-incompetent intermediate ensemble. The fraction of molecules in the population that form these intermediates in the burst phase depends on the relative values of k_1 and k_3 . These rates are much slower than the intrinsic rate for chemical exchange of the probe protons in RNase A (cf. Table 1).

Since no burst phase changes in the CD and tyrosine fluorescence are observed during unfolding, N_1^* and I_U^2 must resemble native RNase A in their secondary and tertiary structures. The rate constants of the structural transition monitored by far-UV CD at 222 nm are faster than those measured by the two probes for tertiary structure. Another intermediate, I_U^3 , which has lost all its native α -helical secondary structure, therefore needs to be invoked on the unfolding route of I_U^2 . It is necessary in the simulation of mechanism 2 to ascribe to I_U^3 only 30% of the native fluorescence and near-UV CD, which are then lost in the final unfolding step from I_U^3 to U_F^* . The nonlinear dependence on GdnHCl concentration of the logarithm of the slow-phase rate constants measured by all three spectroscopic probes also supports the existence of I_U^3 .

The backbone NH protons of class I residues become accessible to exchange with the solvent protons only in the fully exchange-competent unfolded state. The protons belonging to class II residues which are protected in the fraction of molecules that form I_U^2 also become exposed to solvent in U_F^* . Since I_U^3 resembles U_F^* in its far-UV CD, but still has some tertiary interactions and is natively like in its amide exposure, the rate of the observable change of CD at 222 nm will be faster than the rate of change of fluorescence, CD at 275 nm and exposure of the backbone NH protons, if $k_2, k_4 > k_5$.

Mechanism 2 cannot be solved analytically and was therefore tested by kinetic simulation. The kinetic traces obtained for the change in CD and fluorescence, and for change in exposure of backbone NH protons, when unfolding is simulated according to mechanism 2, are shown in Figure 8. The simulation showed that typical proline isomerization rates of 0.02 s^{-1} and 0.004 s^{-1} for the $U_F \rightarrow U_S$ and $U_S \rightarrow U_F$ reactions, respectively, used along with the values of $k_1, k_2, k_3, k_4,$ and k_5 that are listed in the legend to Figure 8, could not only account for the kinetic data but also predicted the known equilibrium ratio of U_F to U_S to be 20:80 (43, 44). The fast phase of unfolding of RNase A observed under these experimental conditions, which is ascribed to the proline isomerization reaction has a rate of 0.023 s^{-1} (see Results). Since $k_4 \approx k_6$, the I_U^2 to I_U^3 step in the structural transition is not distinguishable as a separate phase in the unfolding process. It is seen in Figure 8 that mechanism 2 satisfactorily describes the experimental data. The initial lag of a few seconds observed in the simulation of the accessibility to solvent of class II protons during unfolding cannot be distinguished in the scatter in the HX data.

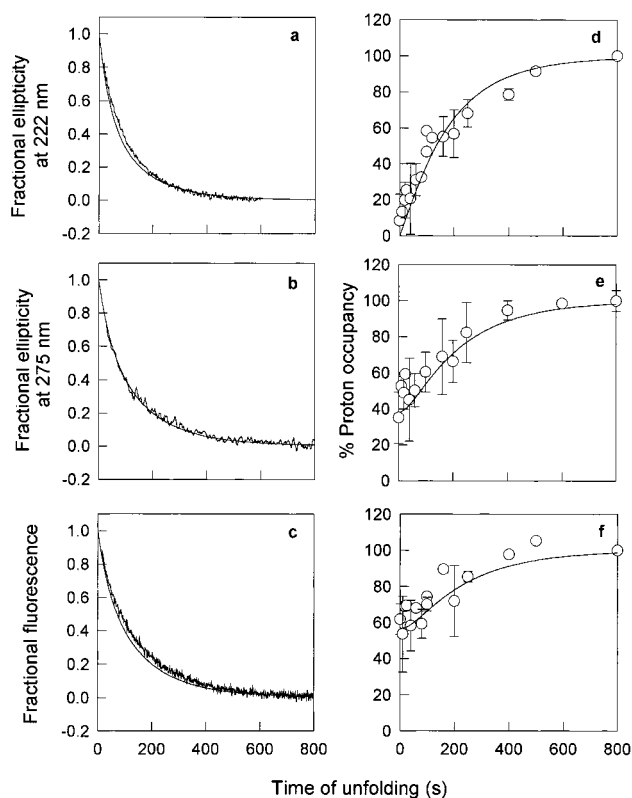


FIGURE 8: Kinetics of unfolding of RNase A in 5.2 M GdnHCl measured by (a) change in ellipticity at 222 nm, (b) change in ellipticity at 275 nm, and (c) change in intrinsic tyrosine fluorescence and kinetics of exposure of (d) class I and (e, f) class II backbone amide protons. (○) Proton occupancies of (d) Cys72, (e) Lys61, and (f) Glu49 at different times of unfolding. The solid lines in all panels are simulations of the experimental data to mechanism 2. The change in CD at 222 and 275 nm, change in tyrosine fluorescence, and the kinetics of exposure of NH probe protons belonging to class I residues on unfolding of RNase A have all been simulated using values of 5 s^{-1} , 0.007 s^{-1} , 4 s^{-1} , 0.025 s^{-1} , 0.005 s^{-1} , 0.02 s^{-1} , and 0.004 s^{-1} for $k_1, k_2, k_3, k_4, k_5, k_6,$ and k_7 , respectively. For the class II NH probe protons, which show 10–40% more labeling at the $t = 0$ unfolding time than in N_1^* under native conditions, the fraction of N molecules unfolding via the N_1^* and the I_U^2 pathways will depend on the relative values of k_1 and k_3 ; for Lys61 the HX data have been simulated using a value of 1.44 s^{-1} for k_1 . For the class II NH probe protons, which show similar extents of labeling in N_1^* under native conditions and at $t = 0$ unfolding time, $k_1 \ll k_3$; for Glu49 the HX data have been simulated using a value of 0.08 s^{-1} for k_1 .

Dissolution of Structure during Unfolding. The data suggest that the backbone NH protons are exposed to exchange with the solvent protons only when the packing interactions in the protein are completely disrupted. This is emphasized by the fact that the 43 amide proton probes, which are distributed in different parts of the protein (Figure 6b), all have virtually the same rate of exposure to exchange (Table 1), which is the same as the rates of change of near-UV CD and intrinsic tyrosine fluorescence of the protein. Most of the hydrogen-bonded protons in RNase A are also the ones which are buried (cf. Table 1). According to mechanism 2, protons in I_U^3 are protected from HX although all of the ellipticity at 222 nm and 70% of both the fluorescence and ellipticity at 275 nm are lost. It appears, however, that water has still not penetrated the core of the protein, so that even though most of the α -helical backbone H-bonds might be broken with the loss of the far-UV CD

signal in I_U^3 , all 43 NH protons remain inaccessible to solvent. In this context, previous one-dimensional ^1H NMR studies of the unfolding of RNase A in 4.5 M GdnHCl at pH 8 and 10 °C had suggested that a dry molten globule intermediate accumulates during unfolding (23). This was based on the observation that the intensity of the $\text{C}'\text{H}_3$ resonance line of Val63 was only 26% of that of the native protein at a certain time of unfolding at which 70% of the molecules were expected to be native according to CD measurements. It was therefore proposed that an unfolding intermediate accumulates in which water has not penetrated the hydrophobic core of the protein although most side chains have become free to rotate.

I_U^3 has the unusual property of being virtually devoid of α -helical secondary structure but still possessing sufficient tertiary interactions to afford 43 amide hydrogens protection from exchange. Twelve of these 43 slowly exchanging amide hydrogens belong to residues found in α -helices in the native protein (cf. Table 1). I_U^3 appears to be a compact form, in which water has not yet penetrated the core of the protein (see above), and such penetration of water is essential for HX to occur. Compact forms of proteins with no specific secondary structure have been observed earlier for apocytochrome *c* (60) and for barstar (61). Moreover, in the unfolding of barstar it has been reported that a burst phase loss in secondary structure is not accompanied by hydration of the core of the protein, which occurs more slowly (26).

CD and HX-Monitored Unfolding Kinetics. According to the experimental data presented here, at least some α -helical secondary structural elements in RNase A appear to break-down before the backbone amides become accessible to hydrogen exchange as the protein unfolds in 5.2 M GdnHCl. In contrast, the rate of unfolding of RNase A in 4.5 M GdnHCl monitored by CD was observed to be less than the rate of HX in the competition labeling experiment reported by Kiefhaber et al. (40). The difference in the rates was attributed to the fact that CD measures an apparent rate constant which includes the microscopic rate constants for unfolding and refolding coupled to the rates for proline isomerization, but in the model for RNase A unfolding proposed in that study it was necessary to propose that the rate of refolding is faster than the rate of unfolding in strong denaturing conditions (40), which is very unlikely.

Folding and Unfolding Studied Using Pulse Labeling by HX. In the EX2 limit of equilibrium HX, protons exchanging by global unfolding may be used as indicators of global stability. It was proposed, on the basis of measurements of HX rates of protons in BPTI, that slow-exchanging protons get protected early on the refolding pathway of the protein (62). Support for this correlation comes from studies on lysozyme (17), cytochrome *c* (36), and RNase T1 (63).

Amide probe protons in an early folding intermediate of RNase A have been classified into three groups on the basis of their protection factors, measured in a refolding study of the protein, using pulse labeling by HX and 2D NMR (35). Val47, His48, Val54, Val63, Cys72, Tyr73, Ile81, Cys84, Lys98, Ile106, Val108, Val116, Val118, and His119 were seen to get strongly protected from exchange in the early folding intermediate. Most of these amides were shown to exchange by global unfolding in a recent study in which HX rates in the EX2 limit were measured for the amide protons and the free energies of exchange for each proton compared

to the free energy of unfolding obtained from calorimetric data (64). Thus, it is not surprising that none of the protons identified in earlier studies as belonging to the most stable regions of RNase A (35, 64–66) show burst phase labeling in the pulsed HX unfolding experiments described here. In contrast, among the protons that do get labeled very rapidly during unfolding, Asn34, Val43, Ser59, and Glu49 have been shown to be weakly or moderately protected from exchange in the early folding intermediate (35). The other protons (except Gln60) known to have moderate protection in the early folding intermediate show an increase in proton occupancy with the length of the exchange pulse in the native-state HX experiments reported in this study (discussed below), although they do not show any burst phase labeling during unfolding. Three of the probe protons, viz., His12 and Met13 in helix 1 and Glu49, were shown to be stabilized only in the final rate-limiting step of folding in the pulsed HX study (35). Here, Gln11 belonging to helix 1 and Asp14, which is in the loop following helix 1, show burst phase exposure to labeling at the start of unfolding. This suggests that the N-terminal helix which is stabilized last during folding is one of the first regions of the protein to get destabilized during unfolding. Glu49 also shows burst phase exposure to labeling in the experiments presented here.

Furthermore, in the equilibrium HX study mentioned above (64), Gln11, Asp14, Val43, Ser59, Lys61, and Glu49 appeared to exchange by small-amplitude local unfolding events, indicating that they belong to considerably less stable regions of RNase A. (The exchange rates for Asn34 and Lys91 were within the dead time of that experiment and could not be measured.) It is therefore possible that because these sites are in regions of the protein which are more labile, they are partially unfolded in some fraction of molecules as soon as the protein encounters strong denaturing conditions. The region from Lys31 to Leu35 in helix 2 (Asn24–Asn34) along with the adjacent β -strand containing Thr45–Phe46 has also been observed to be the first to become susceptible to proteolytic cleavage when the protein is thermally denatured (67). His12, which was observed to be weakly protected (35) and also appeared to exchange by local unfolding events (64), shows $16 \pm 10\%$ labeling at the start of unfolding in the pulsed HX experiments reported here. It has, however, been classified as a class I proton since the extent of labeling lies within the error of measurement in these experiments.

It is interesting to note that, in pulsed HX studies of RNase A folding (35), the earliest detected intermediate is not populated fully when it is first formed, and this observation could not be explained satisfactorily. In the unfolding experiments reported here, the explanation that has been proposed for failure to populate the labeling-competent earliest unfolding intermediate N_I^* fully when it is first formed is that a second intermediate, I_U^2 , forms in competition with N_I^* on a parallel unfolding pathway. It is likely that folding of RNase A also occurs via two competing pathways, and that may be the reason the earliest folding intermediate was observed not to accumulate to the expected extent in the earlier folding studies.

Native-State HX and the Unfolding Mechanism of RNase A. In a previous native-state HX study of RNase A in subdenaturing concentrations of GdnHCl, the *m*-values and free energies evaluated for the conformational reaction that

permits exchange of each of 23 backbone amide protons indicated that the native protein equilibrates with partially unfolded intermediates (68), but it could not be determined if these were on-pathway. For cytochrome *c* (29, 69) and RNase H (30), it has been suggested that the progressively unstructured forms populated at equilibrium in native conditions may represent the hierarchical unfolding pathway of these proteins. In fact, the stabilities of different regions of these proteins evaluated from native-state HX experiments correlate remarkably well with the pattern of protection of amide protons in the kinetic folding intermediates observed by HX. Here, it has been shown that the partially unfolded state, N_I^* , observed in equilibrium native-state HX experiments, also populates one of the unfolding pathways of the predominant native form of RNase A.

ACKNOWLEDGMENT

All NMR spectra were recorded at the NMR facility at TIFR, Mumbai. We thank Sanjay Panchal, Abani Bhuyan, and Neel Sarovar Bhavesh for useful discussions and help with the spectrometer.

REFERENCES

- Bryngelson, J. D., Onuchic, J. N., Socci, N. D., and Wolynes, P. G. (1995) *Proteins: Struct., Funct., Genet.* **21**, 167–195.
- Dill, K. A., and Chan, H. S. (1997) *Nat. Struct. Biol.* **4**, 10–19.
- Chan, H. S., and Dill, K. A. (1998) *Proteins: Struct., Funct., Genet.* **30**, 2–33.
- Pande, V. S., Grosberg, A. Y., Tanaka, T., and Rokhsar, D. S. (1998) *Curr. Opin. Struct. Biol.* **8**, 68–79.
- Englander, S. W., and Mayne, L. (1992) *Annu. Rev. Biophys. Biomol. Struct.* **21**, 243–265.
- Baldwin, R. L. (1993) *Curr. Opin. Struct. Biol.* **3**, 84–91.
- Clarke, J., and Itzhaki, L. S. (1998) *Curr. Opin. Struct. Biol.* **8**, 112–118.
- Englander, S. W. (2000) *Annu. Rev. Biophys. Biomol. Struct.* **29**, 213–238.
- Chamberlain, A. K., and Marqusee, S. (2000) *Adv. Protein Chem.* **53**, 283–328.
- Chan, H. S., and Dill, K. A. (1991) *Annu. Rev. Biophys. Biomol. Struct.* **20**, 447–490.
- Chan, H. S., and Dill, K. A. (1996) *Proteins: Struct., Funct., Genet.* **24**, 335–344.
- Jackson, S. E., and Fersht, A. R. (1991) *Biochemistry* **30**, 10428–10435.
- Huang, G. S., and Oas, T. G. (1995) *Biochemistry* **34**, 3884–3892.
- Schindler, T., Herrler, M., Marahiel, M. A., and Schmid, F. X. (1995) *Nat. Struct. Biol.* **2**, 663–673.
- Udgaonkar, J. B., and Baldwin, R. L. (1988) *Nature* **335**, 694–699.
- Houry, W. A., Rothwarf, D. M., and Scheraga, H. A. (1994) *Biochemistry* **33**, 2516–2530.
- Radford, S. E., Dobson, C. M., and Evans, P. A. (1992) *Nature* **358**, 302–307.
- Miranker, A., Robinson, C. V., Radford, S. E., Aplin, R. T., and Dobson, C. M. (1993) *Science* **262**, 896–900.
- Shastri, M. C., and Udgaonkar, J. B. (1995) *J. Mol. Biol.* **247**, 1013–1027.
- Mark, A. E., and Gunsteren, W. F. (1992) *Biochemistry* **31**, 7745–7748.
- Paci, E., Smith, L. J., Dobson, C. M., and Karplus, M. (2001) *J. Mol. Biol.* **306**, 329–347.
- Cafilisch, A., and Karplus, M. (1994) *Proc. Natl. Acad. Sci. U.S.A.* **91**, 1746–1750.
- Kiefhaber, T., Labhardt, A. M., and Baldwin, R. L. (1995) *Nature* **375**, 513–515.
- Philips, C. M., Mizutani, Y., and Hochstrasser, R. M. (1995) *Proc. Natl. Acad. Sci. U.S.A.* **92**, 7292–7296.
- Hoeltzli, S. D., and Frieden, C. (1995) *Proc. Natl. Acad. Sci. U.S.A.* **92**, 9318–9322.
- Nath, U., Agashe, V. R., and Udgaonkar, J. B. (1996) *Nat. Struct. Biol.* **3**, 920–923.
- Zaidi, F. N., Nath, U., and Udgaonkar, J. B. (1997) *Nat. Struct. Biol.* **4**, 1016–1024.
- Ramachandran, S., Rami, B. R., and Udgaonkar, J. B. (2000) *J. Mol. Biol.* **297**, 733–745.
- Bai, Y., Sosnick, T. R., Mayne, L., and Englander, S. W. (1995) *Science* **269**, 192–197.
- Chamberlain, A. K., Handel, T. M., and Marqusee, S. (1996) *Nat. Struct. Biol.* **3**, 782–787.
- Bhuyan, A. K., and Udgaonkar, J. B. (1998) *Proteins: Struct., Funct., Genet.* **30**, 295–308.
- Goldenberg, D. P., and Creighton, T. E. (1985) *Biopolymers* **24**, 167–182.
- Segawa, S., and Sugihara, M. (1984) *Biopolymers* **23**, 2473–2488.
- Segawa, S., and Sugihara, M. (1984) *Biopolymers* **23**, 2489–2498.
- Udgaonkar, J. B., and Baldwin, R. L. (1990) *Proc. Natl. Acad. Sci. U.S.A.* **87**, 8197–8201.
- Roder, K., Elove, G. A., and Englander, S. W. (1988) *Nature* **335**, 700–704.
- Jennings, P. A., and Wright, P. E. (1993) *Science* **262**, 892–896.
- Raschke, T. M., and Marqusee, S. (1997) *Nat. Struct. Biol.* **4**, 298–304.
- Neira, J. L., and Rico, M. (1997) *Folding Des.* **2**, R1–R11.
- Kiefhaber, T., and Baldwin, R. L. (1995) *Proc. Natl. Acad. Sci. U.S.A.* **92**, 2657–2661.
- Robertson, A. D., Purisima, E. O., Eastman, M. A., and Scheraga, H. A. (1989) *Biochemistry* **28**, 5930–5938.
- Agashe, V. R., and Udgaonkar, J. B. (1995) *Biochemistry* **34**, 3286–3299.
- Rehage, A., and Schmid, F. X. (1982) *Biochemistry* **21**, 1499–1505.
- Garel, J. R., Nall, B. T., and Baldwin, R. L. (1976) *Proc. Natl. Acad. Sci. U.S.A.* **73**, 1853–1857.
- Brandts, J. F., Halvorson, H. R., and Brennan, M. (1975) *Biochemistry* **14**, 4953–4963.
- Schmid, F. X., and Baldwin, R. L. (1978) *Proc. Natl. Acad. Sci. U.S.A.* **75**, 4764–4768.
- Kiefhaber, T., Kohler, H. H., and Schmid, F. X. (1992) *J. Mol. Biol.* **224**, 217–229.
- Kiefhaber, T., and Schmid, F. X. (1992) *J. Mol. Biol.* **224**, 231–240.
- Parker, M. J., Spencer, J., and Clarke, A. R. (1995) *J. Mol. Biol.* **253**, 771–786.
- Oliveberg, M., Tan, Y.-J., Silow, M., and Fersht, A. R. (1998) *J. Mol. Biol.* **277**, 933–943.
- Otzen, D. E., Kristensen, O., Proctor, M., and Oliveberg, M. (1999) *Biochemistry* **38**, 6499–6511.
- Silow, M., and Oliveberg, M. (1997) *Biochemistry* **36**, 7633–7637.
- Santoro, J., Gonzalez, C., Bruix, M., Neira, J. L., Nieto, J. L., Herranz, J., and Rico, M. (1993) *J. Mol. Biol.* **229**, 722–734.
- Rico, M., Santoro, J., Gonzalez, C., Bruix, M., Neira, J. L., Nieto, J. L., and Herranz, J. (1991a) *J. Biomol. NMR* **1**, 283–298.
- Shimotakahara, S., Rios, C. B., Laity, J. H., Zimmerman, D. E., Scheraga, H. A., and Montelione, G. T. (1997) *Biochemistry* **36**, 6915–6929.

56. Barshop, A., Wrenn, R. F., and Frieden, C. (1983) *Anal. Biochem.* 130, 134–145.
57. Loh, S. N., Rohl, C. A., Kiefhaber, T., and Baldwin, R. L. (1996) *Proc. Natl. Acad. Sci. U.S.A.* 93, 1982–1987.
58. Kiefhaber, T., and Baldwin, R. L. (1996) *Biophys. Chem.* 59, 351–356.
59. Kim, P. S. (1986) *Methods Enzymol.* 131, 136–156.
60. Hamada, D., Hoshino, M., Kataoka, M., Fink, A. L., and Goto, Y. (1993) *Biochemistry* 32, 10351–10358.
61. Agashe, V. R., Shastry, M. C., and Udgaonkar, J. B. (1995) *Nature* 377, 754–757.
62. Kim, K. S., Fuchs, J. A., and Woodward, C. K. (1993) *Biochemistry* 32, 9600–9608.
63. Mullins, L. S., Pace, C. N., and Raushel, F. M. (1997) *Protein Sci.* 6, 1387–1395.
64. Neira, J. L., Sevilla, P., Menendez, M., Bruix, M., and Rico, M. (1999) *J. Mol. Biol.* 285, 627–643.
65. Wang, A., Robertson, A. D., and Bolen, D. W. (1995) *Biochemistry* 34, 15096–15104.
66. Chakshusmathi, G., Ratnaparkhi, G. S., Madhu, P. K., and Varadarajan, R. (1999) *Proc. Natl. Acad. Sci. U.S.A.* 96, 7899–7904.
67. Arnold, U., Rücknagel, K. P., Schierhorn, A., and Ulbrich-Hofmann, R. (1996) *Eur. J. Biochem.* 237, 862–869.
68. Mayo, S. L., and Baldwin, R. L. (1993) *Science* 262, 873–876.
69. Milne, J. S., Xu, Y., Mayne, L. C., and Englander, S. W. (1999) *J. Mol. Biol.* 290, 811–822.
70. Lee, B., and Richards, F. M. (1971) *J. Mol. Biol.* 55, 379–400.
71. Bai, Y., Milne, J. S., Mayne, L., and Englander, S. W. (1993) *Proteins: Struct., Funct., Genet.* 17, 75–86.

BI011480P